The SAND domain protein ULTRAPETALA1 acts as a trithorax group factor to regulate cell fate in plants

Cristel C. Carles[1] and Jennifer C. Fletcher[2]

Plant Gene Expression Center, United States Department of Agriculture/University of California at Berkeley, Albany, California 94710, USA; Department of Plant and Microbial Biology, University of California at Berkeley, Berkeley, California 94720, USA

During development, trithorax group (trxG) chromatin remodeling complexes counteract repression by Polycomb group (PcG) complexes to sustain active expression of key regulatory genes. Although PcG complexes are well characterized in plants, little is known about trxG activities. Here we demonstrate that the *Arabidopsis* SAND (Sp100, AIRE-1, NucP41/75, DEAF-1) domain protein ULTRAPETALA1 (ULT1) functions as a trxG factor that counteracts the PcG-repressive activity of CURLY LEAF. In floral stem cells, ULT1 protein associates directly with the master homeotic locus *AGAMOUS,* inducing its expression by regulating its histone methylation status. Our analysis introduces a novel mechanism that mediates epigenetic switches controlling post-embryonic stem cell fates in plants.

Supplemental material is available at http://www.genesdev.org.

Received August 4, 2009; revised version accepted October 14, 2009.

Plants generate their reproductive organs late in development through the formation of flowers. This establishes a requirement for the repression of key floral homeotic genes during vegetative development and their subsequent tissue-specific activation during the reproductive stage. In *Arabidopsis thaliana*, ULTRAPETALA1 (ULT1) is essential to terminate stem cell activity in the center of the flower meristem through the timely activation of the floral homeotic gene *AGAMOUS* (*AG*) (Fletcher 2001; Carles et al. 2004). *AG* encodes a MADS (MCM1, AGAMOUS, DEFICIENS, SRF) domain transcription factor that specifies reproductive organ identity (Bowman et al. 1989) and acts in a negative feedback loop to limit floral stem cell proliferation (Lenhard et al. 2001; Lohmann et al. 2001; Sun et al. 2009). *ULT1* is expressed early during floral meristem initiation (Carles et al. 2005) and is required to activate *AG* expression at the correct stage of floral development, thus acting as a critical temporal component of the floral meristem termination pathway.

[*Keywords*: Stem cell; epigenetics; chromatin; trithorax group; Polycomb group; gene activation]

[1]**Present address: Laboratoire de Physiologie Cellulaire Végétale, Université de Grenoble, UMR5168, CNRS-CEA-INRA1200-UJF, CEA, 17 rue des Martyrs, bât. C2, 38054 Grenoble Cedex 9, France.**
[2]**Corresponding author.**
E-MAIL fletcher@nature.berkeley.edu; FAX (510) 559-5678.
Article is online at http://www.genesdev.org/cgi/doi/10.1101/gad.1812609.

Maintenance of the appropriate *AG* transcriptional status in nonreproductive versus reproductive tissues involves the opposite activities of Polycomb group (PcG) and trithorax group (trxG) chromatin remodeling factors. The PcG gene *CURLY LEAF* (*CLF*), a homolog of the *Drosophila Enhancer of zeste E(z)* histone methyltransferase, acts as a component of Polycomb-Repressive Complex PRC2 (Chanvivattana et al. 2004). CLF is a direct transcriptional repressor of *AG* expression in leaves, inflorescences, and the outer whorls of flowers (Goodrich et al. 1997) that mediates trimethylation of histone 3 Lys 27 (H3K27me3) (Schubert et al. 2006). Conversely, *ARABIDOPSIS HOMOLOG OF TRITHORAX1* (*ATX1*), a homolog of *Drosophila trithorax*, encodes a histone methyltransferase for trimethyl groups on histone 3 Lys 4 (H3K4me3) (Alvarez-Venegas et al. 2003; Alvarez-Venegas and Avramova 2005; Saleh et al. 2007) that sustains high-level *AG* transcription in flowers (Alvarez-Venegas et al. 2003). These proteins maintain the *AG* locus in either a repressed or an active state in a tissue-specific fashion, yet nothing is known about the epigenetic factors that mediate the *AG* switch from a repressed to an active state within the floral stem cell reservoir. Nor is it understood through what mechanism the ULT1 protein, which contains a putative DNA-binding SAND (Sp100, AIRE-1, NucP41/75, DEAF-1) domain (Bottomley et al. 2001) but no evident transcription activation domain, functions in the floral stem cell termination pathway.

Results and Discussion

ULT1 gain-of-function phenotypes resemble those of 35S::AG and clf plants

To gain insight into the mechanism of ULT1 transcriptional control, we expressed *ULT1* from the constitutively active cauliflower mosaic virus (CaMV) 35S promoter in transgenic *Arabidopsis* plants. The *35S::ULT1* transgenic plants displayed small rosettes and upward-curled rosette leaves, as well as early flowering, short stature, increased branch outgrowths, and prematurely terminating inflorescence meristems (Fig. 1A–D). The plants produced small flowers with mosaic organs; notably, carpeloid sepals and stamenoid petals (Fig. 1D; Supplemental Fig. S1A–E). RT–PCR showed that the severity of the phenotypes strongly correlated with the level of *ULT1* overexpression (Fig. 1B); severely affected class 1 *35S::ULT1* plants were used for further analysis.

The *35S::ULT1* phenotypes resembled those of *35S::AG* plants (Mizukami and Ma 1992) and of loss-of-function *clf* plants, which ectopically express *AG* and *APETALA3* (*AP3*) in leaves and flowers (Figs. 1, 2A,H; Supplemental Fig. S2A; Goodrich et al. 1997). *AG* and *AP3* transcripts accumulated ectopically in *35S::ULT1* rosette leaves and inflorescence meristems, as well as in sepals and carpels, respectively (Fig. 1E,F). Thus, ULT1 can induce *AG* expression, consistent with previous results showing that *AG* induction is delayed in the center of *ult1* floral meristems (Fletcher 2001). Introduction of the *35S::ULT1* construct into either the *ag-3* or the *ap3-3* background demonstrated that the 35S::*ULT1* phenotypes, like the *clf* phenotypes (Goodrich et al. 1997), were dependent primarily on ectopic *AG* activity

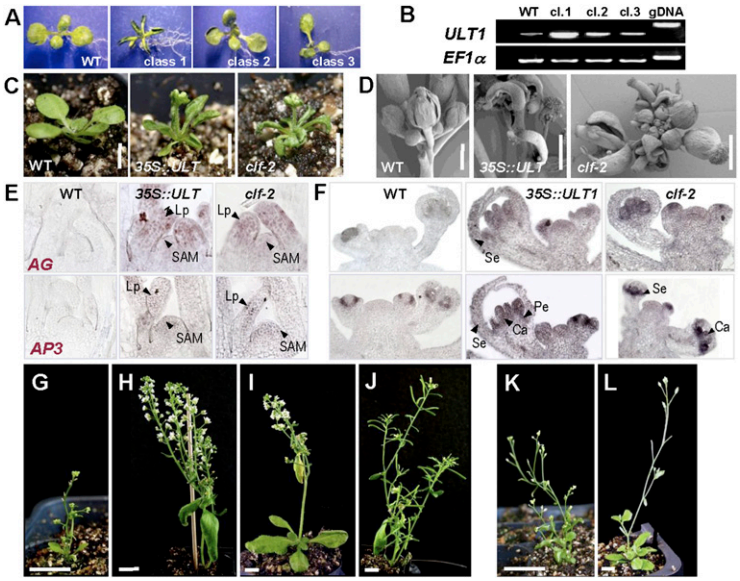

Figure 1. *35S::ULT1* transgenic plants resemble *clf* plants and ectopically activate *AG* and *AP3*. (*A*,*B*) Correlation between *35S::ULT1* phenotype severity and *ULT1* expression levels. (*A*) Population classes range from most (class 1) to least (class 3) severe. (WT) Wild type. (*B*) RT–PCR with seedling RNA from wild-type and class 1 to class 3, using *EF1α* as the reference gene. (gDNA) Genomic DNA control. (*C*,*D*) *35S::ULT1* vegetative and inflorescence phenotypes resemble those observed in *clf* plants. (*C*) Fifteen-day-old plantlets on soil. (*D*) Scanning electron micrographs of inflorescences. (*E*,*F*) RNA in situ hybridization showing ectopic expression of *AG* and *AP3* in seedlings (*E*) and inflorescences (*F*) of wild-type, *35S::ULT1*, and *clf-2* plants. (SAM) Shoot apical meristem; (Lp) leaf primordium; (Se) sepal primordium; (Pe) petal primordium; (Ca) carpel primordium. (*G–L*) Segregating T3 descendents of a *35S::ULT1; ag-3*/+ plant. (*G*) *35S::ULT1 AG*/*AG* plant. (*H*) *35S::ULT1 ag-3*/*ag-3* plant. (*I*) *ag-3*/*ag-3* plant. (*J*) Wild-type plant. (*K*) *35S::ULT1; ap3-3* plant. (*L*) *ap3-3* plant. Bars: *C*, 5 mm; *D*, 1 mm; *G–L*, 1 cm.

(Fig. 1G–J; Supplemental Fig. S1F–I). However, the *35S::ULT1* phenotypes also depended to a lesser extent on *AP3* activity (Fig. 1K,L).

Additional ULT1 regulatory targets were identified by RT–PCR analysis. The *AG*-related MADS-box genes *SEP1*, *SEP2*, and *SEP4* were strongly up-regulated in *35S::ULT1* plants, while *SEP3* expression was weakly elevated (Supplemental Fig. S2A). These four *SEP* genes were also up-regulated in *clf-2* plants (Supplemental Fig. S2A). *SEP* gene activation may reflect a secondary effect of *AG* ectopic expression because these genes, as well as *AP3*, are targets of AG transcriptional regulation (Gomez-Mena et al. 2005). Expression of the floral activator *AGL19* was unaltered in *35S::ULT1* leaves (Supplemental Fig. S2A), indicating that ULT1 shows specificity in regulating MADS-box gene expression. We also observed ectopic activation of the class I *KNOX* homeobox gene *STM* and up-regulation of the related *BP*, *KNAT2*, and *KNAT6* genes in *35S::ULT1* and *clf-2* leaves (Supplemental Fig. S2B). These data indicate a substantial degree of overlap between genes positively regulated by ULT1 and genes negatively regulated by CLF. CLF and ULT1 do not significantly regulate one another's transcription (Supplemental Fig. S2C), nor is the *CLF* expression pattern altered in *35S::ULT1* inflorescence tissue (Supplemental Fig. S3). These data are inconsistent with *ULT1* being a downstream target of CLF or vice versa, or ULT1 inhibiting the activity of the *CLF* locus, but instead suggest that ULT1 and CLF oppositely regulate a common set of target genes.

ULT1 displays a genetic trxG function

To determine the genetic relationship between *ULT1* and *CLF*, we generated *ult1 clf-2* double mutants. Three different *ult1* mutant alleles independently rescued all *clf-2* vegetative and reproductive defects (Fig. 2A–C; Supplemental Fig. S4). These results show that *clf* phenotypes are totally dependent on ULT1 activity, and indicate that ULT1 and CLF have opposite, possibly antagonistic, effects on plant development. *Drosophila* genes belonging to the trxG were originally identified as suppressors of PcG mutant phenotypes (Ingham 1988; Kennison 1995). Because *ult1* mutations were able to completely suppress all PcG *clf-2* mutant phenotypes, *ULT1* meets the genetic definition of a trxG gene.

We investigated the *ult1*-mediated suppression of the *clf-2* phenotypes by examining expression levels of the key CLF target gene, *AG*. Compared with *clf* rosette leaves, *ult1 clf* rosette leaves displayed much lower levels of ectopic *AG* expression (Fig. 2D), and these levels were insufficient to induce the *clf* phenotype. Similarly, *ult1 clf* stage 3 floral buds accumulated *AG* mRNA at much lower levels than *clf* stage 3 floral buds, and in a pattern similar to *ult1* stage 3 floral buds (Fig. 2E–G; Fletcher 2001). We observed that the expression levels of the *AG* downstream target genes *AP3*, *SEP1*, *SEP2*, *SEP3*, and *SEP4* were also reduced in *ult1 clf* plants compared with *clf* plants (Supplemental Fig. S5), likely contributing to the rescue of the *clf* phenotypes by mutations in *ult1*. Conversely, the timing of *AG* activation in the center of *ult1* floral meristems was not affected by the *clf* mutation. In wild-type and *clf-2* floral buds, *AG* was expressed throughout the central dome by stage 3 (Fig. 2F; Goodrich et al. 1997), whereas the onset of *AG* expression was delayed in the center of both *ult1* (Fig. 2E) and *ult1 clf* (Fig. 2G) floral meristems.

We next determined whether ectopic induction of *AG* target genes in *35S::AG* plants was impaired by mutations in *ULT1*. We observed that *35S::AG ult1* rosette leaves displayed wild-type morphology (Fig. 2H–J) and had reduced total *AG* mRNA levels relative to *35S::AG* lines containing functional *ULT1* (Fig. 2K). Moreover, loss of ULT1 activity rescued the *35S::AG* phenotypes in a dosage-dependent fashion, because *35S::AG ult1-3*/+ plants displayed developmental and molecular phenotypes intermediate between those of *35S::AG* and *35S::AG ult1-3* plants (Fig. 2H–K). Whereas the *ult1* mutation did not impair *AG* transgene expression in *35S::AG* plants, ULT1 was required to sustain autoactivation (Gomez-Mena et al. 2005) of the endogenous *AG* locus (Fig. 2L). This result indicates that ULT1 regulation of *AG* requires the native regulatory sequence and/or chromatin configuration. In addition, ectopic *AG* induction of *AP3* but not *SEP3* was dependent on ULT1 (Fig. 2L). ULT1 activity is therefore required for maximal expression of *AG* as well as of some *AG* target genes.

The effect of ULT1 on *AG* and *AP3* transcription levels was confirmed by quantitative real-time PCR (Fig. 3A). In wild-type and *ult1* seedlings, *AG* and *AP3* expression was

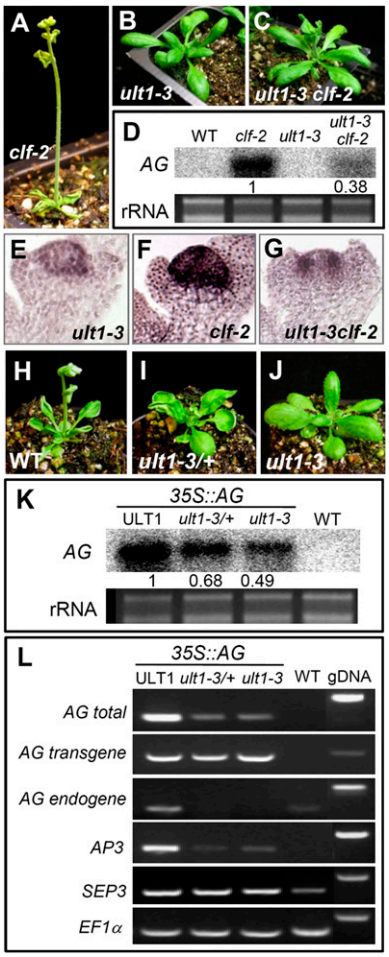

Figure 2. ULT1-dependent expression of phenotypes caused by *AG* ectopic activation. (*A–C*) *clf-2* phenotypes are rescued in an *ult1-3*-null mutant background. (*D*) RNA blot of rosette leaf tissue showing reduction in *clf*-induced ectopic *AG* expression in 10-d-old *clf-2 ult1-3* plants. The relative amount of *AG* transcript accumulation is indicated, normalized to rRNA. (*E–G*) RNA in situ hybridization showing expression of *AG* in stage 3 floral buds of *ult1-3*, *clf-2*, and *ult1-3 clf-2* plants. (*H–J*) Loss of ULT1 rescues *35S::AG* phenotypes in a dosage-dependent fashion. Plants shown are *35S::AG* transgenic in a wild-type (WT), *ult1-3/ULT1* heterozygous (*ult1-3*/+), or *ult1-3* homozygous (*ult1-3*) background. (*K*) RNA blot of rosette leaf tissue showing *ult1*-induced reduction of ectopic *AG* expression in 28-d-old *35S::AG* plants. The relative amount of *AG* transcript accumulation is indicated, normalized to rRNA. (*L*) RT–PCR with leaf RNA of 28-d-old plants. Primers were used to detect total *AG* mRNA, *AG* mRNA from the *35S::AG* transgene, *AG* mRNA from the endogenous locus, *AP3* mRNA, and *SEP3* mRNA. *EF1α* is shown as the reference gene. Identical results were obtained in experiments using the independent *ult1-1* and *ult1-2* alleles.

barely detectable, whereas *AG* expression was dramatically elevated in *clf* seedlings. In *ult1 clf* seedlings, *AG* transcript levels were reduced by 80% relative to *clf* seedlings, confirming that ULT1 activity is required to obtain high levels of *AG* expression in *clf* seedlings. Surprisingly, *AG* transcription levels in *35S::ULT1* plants were very similar to those in *ult1 clf* plants, despite the fact that *35S::ULT1* seedlings had strong curly leaf phenotypes (Fig. 1A,C), whereas *ult1 clf* seedlings had normal leaf morphology (Fig. 2C). This discrepancy can be explained by the observation that *AP3* expression levels are far higher in *35S::ULT1* seedlings than in *ult1 clf* seedlings (Fig. 3A), and *AP3* contributes to the *35S::ULT1* curly leaf phenotype (Fig. 1K,L). We therefore propose that extremely high-level ectopic expression of *AP3*, as well as other downstream effectors of AG activity such as *SEP1* and *SEP3* (Supplemental Fig. S2), is sufficient to cause a curly leaf phenotype in *35S::ULT1* plants, whereas their ectopic expression at much lower levels in *ult1 clf* plants fails to condition the phenotype.

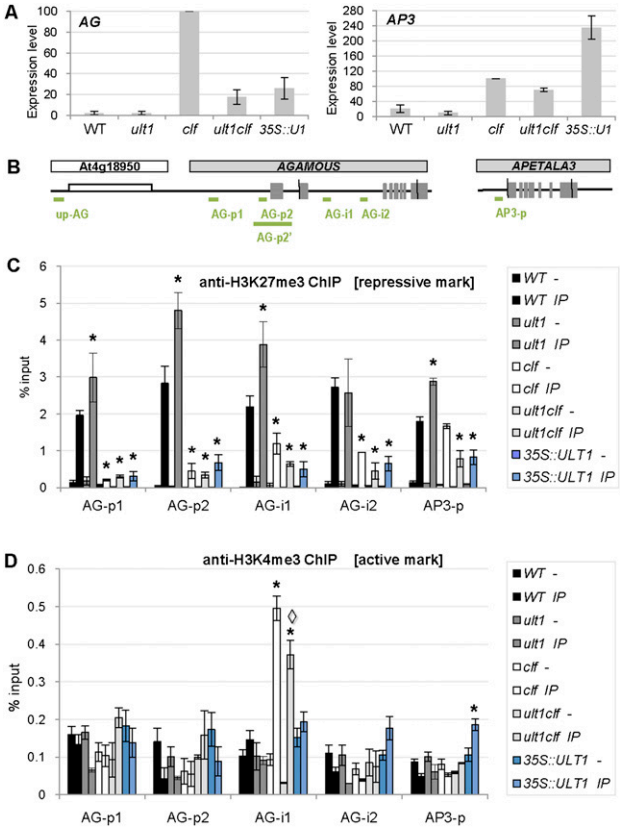

Figure 3. Influence of ULT1 and CLF on *AG* and *AP3* expression levels and histone methylation patterns. (*A*) RT–qPCR analysis of *AG* and *AP3* expression levels in 4-d-old wild-type, *ult1-3*, *clf-2*, *ult1-3 clf-2*, and *35S::ULT1* seedlings. Graphs represent average values from two biological replicates, each standardized to *EF1α*, with the value in the *clf* background set at 100%. Error bars represent standard error. (*B*) Schematic structures of the *AG* locus, *AG* 5′-flanking region, and *AP3* locus. For *AG* and *AP3*, the exon/intron structure is depicted, with the exons as gray boxes. The transcribed region of the upstream At4g18950 gene is indicated (white box). Green lines denote the regions amplified by qPCR for ChIP analysis. (*C*,*D*) H3K27me3 and H3K4me3 patterns at the *AG* and *AP3* loci. ChIP was analyzed by qPCR and results are presented as percentage of input chromatin. Graphs represent average values from two biological replicates. For each locus of interest, the amplification was standardized to the amplification obtained from the region upstream of *AG* (up-AG). Minus sign (–) indicates ChIP minus antibody and IP indicates ChIP plus antibody. Each set of bars in one color represents minus (–) and IP for the same genotype. Error bars represent standard error. Asterisks (*) indicate values that are significantly different from wild type ($P < 0.05$ using Student's *t*-test), and the diamond (◇) indicates that the value for *ult1 clf* is significantly different from *clf* ($P < 0.05$ using Student's *t*-test).

ULT1 activates the AG *locus by controlling its histone methylation status*

A genetic trxG function for ULT1 suggested that it may regulate *AG* expression through chromatin modifications. We tested this hypothesis by analyzing the distribution of histone H3 lysine methylation marks within the promoter and second intron of *AG* (Fig. 3), regions necessary for the correct spatial and temporal regulation of the gene (Sieburth and Meyerowitz 1997). In seedlings, these regions of the silent *AG* locus (Fig. 3A,B) carry the H3K27me3-repressive mark deposited by CLF (Schubert et al. 2005).

Comparisons of chromatin immunoprecipitation (ChIP) profiles of wild-type, *ult1-3*, and *35S::ULT1* seedlings showed alterations in the deposition of the H3K27me3-repressive mark (Fig. 3C). In *ult1-3* seedlings, a 50% to 77% gain in the H3K27me3 mark occurred at the AG-p1, AG-p2, and AG-i1 locations (Fig. 3C). Conversely, in *35S::ULT1* seedlings, we observed a significant loss of the H3K27me3 mark at all four locations tested. These data indicate that ULT1 limits the deposition of H3K27me3-repressive marks at the *AG* locus. The *AG* locus in *35S::ULT1* seedlings carried a similar level of the active H3K4me3 mark as wild-type seedlings (Fig. 3D) but a reduced amount of the repressive H3K27me3 mark, indicating that the locus was shifted toward a more active state, in accordance with the observation that *35S::ULT1* seedlings have higher *AG* transcript levels than wild-type seedlings (Fig. 3A). In *35S::ULT1* seedlings, the repressive mark was lost even though wild-type CLF activity was still present, demonstrating that excess or ectopic ULT1 is sufficient to prevent deposition of repressive marks by CLF. These results are consistent with ULT1 functioning as an trxG anti-repressor that counteracts PcG-mediated transcriptional silencing, as has been proposed for the *Drosophila* trxG proteins Trx and Ash1 (Klymenko and Muller 2004; Papp and Muller 2006).

In agreement with previous reports (Goodrich et al. 1997; Chanvivattana et al. 2004), we found that, in *clf-2* seedlings, *AG* expression was highly elevated (Fig. 3A), and that the *AG* locus was depleted of the H3K27me3-repressive mark in the promoter and second intron (Fig. 3C). Comparison of the H3K27me3-repressive mark in *ult1-3*, *clf-2*, and *ult1-3 clf-2* seedlings indicated that *clf-2* was epistatic to *ult1-3* (Fig. 3C), because in *clf-2* plants, *AG* was depleted of H3K27me3 regardless of the presence or absence of ULT1. In *clf-2* seedlings, the *AG* second intron was also enriched for the H3K4me3 activation mark relative to wild-type seedlings (Fig. 3D). However, deposition of H3K4me3 within the second intron decreased by 26% in *ult1-3 clf-2* seedlings compared with *clf-2* seedlings (Fig. 3D). Thus, although the *AG* locus was depleted of H3K27me3 in *clf-2* seedlings, the absence of ULT1 resulted in modest additional locus-specific depletion of H3K4me3. This reduction in the H3K4me3 activation mark may contribute to the decrease in *AG* transcript levels detected in *ult1-3 clf-2* seedlings (Fig. 3A), as the ratio of the two histone marks is shifted toward a less active state. In contrast to *clf-2* seedlings, *35S::ULT1* seedlings did not show increased deposition of H3K4me3-activating marks at the *AG* locus (Fig. 3D). A possible reason for this is that ULT1 does not itself have H3K4me3 methyltransferase activity, but rather interacts with such an enzyme as part of a trxG complex, and that the relative abundance of this associated H3K4me3 methyltransferase is rate-limiting in seedlings.

Several additional observations are in accordance with *ULT1* not only functioning as an anti-repressor, but also playing a limited role in switching the *AG* locus to an activated state. First, *ult1* flowers, like weak *ag* flowers, produce a fifth whorl of stamen and/or carpel organs (Fletcher 2001), and this fifth whorl activity is still observed in *ult1 clf* flowers (Supplemental Table S1). Second, *AG* is induced normally in the central domain of stage 3 *clf* floral meristems, but is absent from the center of *ult1* and *ult1 clf* floral meristems (Fig. 2E–G; Fletcher 2001). These data demonstrate that even in the absence of the repressive marks, ULT1 is still required for *AG* to be transcribed at the correct time during floral meristem development. Taken together, our results suggest that, in addition to restricting the deposition of H3K27 methylation marks at the *AG* locus by CLF, ULT1 may also play a role in recruiting proteins responsible for local H3K4 methylation and subsequent transcription elongation.

Finally, because *AP3* expression levels were exceedingly high in *35S::ULT1* seedlings compared with wild-type and *clf* seedlings (Fig. 3A), we analyzed the H3 lysine methylation marks at the *AP3* promoter. We found that H3K27me3-repressive marks were significantly reduced and H3K4me3-activating marks were significantly increased in *35S::ULT1* seedlings compared with wild-type or *clf* seedlings (Fig. 3C,D). A likely explanation for the observation that *AP3* expression levels are higher in *35S::ULT1* than in *clf* tissues is that both *AG* and *ULT1* play a role in inducing *AP3* transcription. This is consistent with the reduction of *AP3* expression in *ult1* compared with wild-type plants and in *ult1 clf* compared with *clf* plants (Fig. 3A). Thus, we propose that the dramatically increased *AP3* transcription levels in *35S::ULT1* plants are a combined effect of an altered ratio of repressive to activating chromatin marks at the *AP3* locus, mediated via elevated *ULT1* expression, and elevated expression of *AG,* a transcriptional activator of *AP3* (Gomez-Mena et al. 2005).

ULT1 associates with the AG *locus and physically interacts with ATX1*

To determine which regions of the *AG* locus were required for responsiveness to ULT1-mediated transcriptional activation, we analyzed the expression patterns of combinations of *AG* promoter and second intron sequences driving a β-glucuronidase (GUS) reporter. Both the promoter and the second intron were necessary for ectopic *AG* activation in *35S::ULT1* seedlings and inflorescences (Fig. 4A). To assess whether ULT1 could interact directly with these *AG* regulatory sequences, we generated *35S::ULT1-HA; ult1* transgenic plants and performed ChIP assays on chromatin extracted from rescued *ult1* plants with wild-type phenotypes. We found that ULT1 associated in vivo with specific *AG* regulatory sites located in the promoter-proximal region and in the second intron (Fig. 4B). Thus, *AG* is a direct target of ULT1 regulation. Interestingly, we found that ULT1 has the strongest affinity for a region of the *AG* locus that is slightly downstream from the area carrying enhanced local H3K4me3 in *clf* plants (Fig. 3D). Physical separation of trxG-binding sites from regions of maximal H3K4me3 has also been reported for the animal trxG factor Ash1 (Papp and Muller 2006).

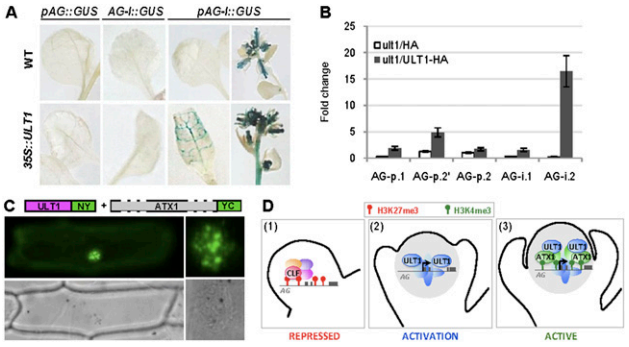

Figure 4. ULT1 associates with the *AG* locus and physically interacts with ATX1. (*A*) *GUS* reporter activity driven by various *AG* regulatory sequences in the presence or absence of *35S::ULT1*. In wild-type plants, *pAG-I::GUS* activity was restricted to floral organs. In *35S::ULT1* plants, ectopic *pAG-I::GUS* activity was detected in rosette leaves and inflorescences. (*B*) Quantification of ULT1 association with *AG* promoter and second intron sequences by ChIP analysis. qPCR values are presented as fold change relative to the *AG* upstream region (up-AG). Error bars represent standard error. *ult1*/HA represents the *ult1-2* mutant expressing a HA tag; *ult1*/ULT1-HA represents the *ult1-2* mutant expressing an ULT1-HA fusion. (*C*) Bimolecular fluorescence complementation assay in which the green signal indicates physical interaction between the ULT1-NY and ATX1-YC fusion proteins inside the nucleus. The *right* image illustrates the subnuclear pattern of the interaction, and the *bottom* images show the bright-field exposure of the transformed cell. (NY) N-terminal half of YFP; (YC) C-terminal half of YFP. (*D*) Mechanistic model for ULT1 regulation of the *AG* locus. (Panel *1*) Floral buds at stage 2, when *AG* repression is maintained by PcG-mediated CLF deposition of H3K27me3 marks. (Panel *2*) At stage 3, the *AG* locus undergoes activation, with ULT1 protein functioning as an anti-repressor to antagonize PcG-induced histone methylation. (Panel *3*) At later stages, *AG* transcription is maintained by trxG activity, as ULT1 associates with ATX1, which deposits H3K4me3 marks.

The ability of ULT1 to affect histone methylation patterns at the *AG* locus suggested the potential for ULT1 to physically interact with the ATX1 trxG factor. Indeed, the two proteins showed a strong interaction in the plant nucleus (Fig. 4C; Supplemental Fig. S6), with a subnuclear localization pattern similar to those of chromatin remodeling proteins (Hernandez-Munoz et al. 2005; Calonje et al. 2008). A comparable pattern was reported for the mammalian SAND domain protein AIRE1, a transcriptional activator of tissue-specific genes in the thymus (Pitkänen et al. 2000; Ferguson et al. 2008). This result, together with the methylation mark analyses, indicates that, in addition to restricting the extent to which H3K27 methylation marks are deposited at the *AG* locus by PcG proteins, ULT1 also associates with proteins such as ATX1 that are responsible for local H3K4 methylation (Alvarez-Venegas et al. 2003). ATX1 is unlikely to be the only factor responsible for H3K4me3 deposition at the *AG* locus, for several reasons. First, *atx1*-null mutants display only weak floral homeotic defects and do not show floral meristem indeterminacy phenotypes characteristic of *ag* flowers (Alvarez-Venegas et al. 2003). Second, 85% of genome-wide H3K4me3 is still present in *atx1* plants (Alvarez-Venegas and Avramova 2005), indicating that additional methyltransferases are likely to play key roles in this process, potentially including other members of the ATX1 family (Alvarez-Venegas and Avramova 2002).

Mechanistic model for activation of the AG *locus*

Together, our data identify the SAND domain protein ULT1 as a trxG factor that binds to *AG* regulatory sequences during flower development and that regulates the deposition of the epigenetic marks, preventing inappropriate PcG silencing of the *AG* locus in the center of the flower, where it must become transcriptionally active (Fig. 4D). During the switch of the *AG* locus from a repressed to an active state, ULT1 may function as a coactivator to recruit additional trxG proteins such as ATX1 that, by analogy with animal systems (Schuettengruber et al. 2007, 2009), are involved in subsequent local H3K4 methylation and/or reading of the chromatin marks for transcription initiation and elongation (Petruk et al. 2006; Li et al. 2007).

Conclusion

Flexible regulation of gene expression through chromatin remodeling is critical for the correct development of eukaryotic organisms, and may be the source of plant developmental plasticity (Pfluger and Wagner 2007). Whereas PcG-mediated repression is considered to be very stable in animal systems, it is often reversible in plants, allowing rapid and dynamic responses to environmental stimuli or developmental cues (Pien et al. 2008). The plasticity of plant cell fate highlights the importance of plant trxG factors that counteract PcG complex repression and promote target gene transcription in a spatially and temporally restricted manner. Identification of the trxG activity of the *Arabidopsis* SAND domain protein ULT1 expands the repertoire of epigenetic regulators of development and uncovers a chromatin-mediated pathway controlling the dynamic switch of transcriptional states that occurs in floral stem cells. It also suggests a molecular mechanism for the activity of animal SAND domain proteins such as AIRE and Sp100, two transcriptional activators associated with human autoimmune regulation (Gibson et al. 1998; Bloch et al. 2000).

Materials and methods

All *Arabidopsis thaliana* genotypes were in the Landsberg *erecta* (L*er*) ecotype and were grown on either Murashige and Skoog medium or soil under continuous light. RNA extraction and RT–PCR were performed as described previously (Carles et al. 2005). Quantification of *AG* and *AP3* cDNAs by real-time PCR was performed using the SYBR Green PCR master mix (Applied Biosystems) and an ABI 7000 Thermocycler (Applied Biosystems). RNA blot hybridization was conducted using a ^{32}P-labeled DNA probe corresponding to the full-length *AG* ORF. For RNA in situ hybridization, *AG* and *AP3* antisense probes were generated using a digoxigenin-labeling mix (Roche). ChIP was performed following a procedure detailed in the Supplemental Material. Immunoprecipitated DNA was analyzed by real-time PCR, and relative enrichments were calculated as the percentage of the obtained values for the immunoprecipitated and input fractions. Bimolecular fluorescence complementation assays were conducted in onion epidermal cells after transformation by particle bombardment using a Biolistic PDS-1000/He unit (Bio-Rad). Epidermal peels were visualized 24 and 36 h after bombardment using a Zeiss Axiophot microscope. Further details and other methods can be found in the Supplemental Material.

Acknowledgments

We thank Chris Day, Justin Goodrich, Bassem Al Sady, Zoya Avramova, Ivan Ndamukong, and Ian Small for materials and constructs. We are grateful to Daniel Schubert and Justin Goodrich for communicating

primer sequences, Elisa Fiume and Erin Osborne for assistance with phenotypic analysis, and Sasha Preuss for insights about the ChIP procedure. We thank Renee Sung, Sheila McCormick, Sarah Hake, Vincent Colot, François Roudier, Robert Blanvillain, and members of the Fletcher laboratory for critical reading of the manuscript. We acknowledge Syngenta, the Salk Institute for Biological Studies, and the *Arabidopsis* Biological Resource Center for providing clones and insertion lines. This work was supported by the National Science Foundation (IBN-0110667).

References

Alvarez-Venegas R, Avramova Z. 2002. The SET-domain proteins of the Su(var)3-9, E(z), and Trithorax families. *Gene* **285:** 25–37.

Alvarez-Venegas R, Avramova Z. 2005. Methylation patterns of histone H3 Lys 4, Lys 9 and Lys 27 in transcriptionally active and inactive *Arabidopsis* genes and in *atx1* mutants. *Nucleic Acids Res* **33:** 5199–5207.

Alvarez-Venegas R, Pien S, Sadder M, Witmer X, Grossniklaus U, Avramova Z. 2003. ATX-1, an *Arabidopsis* homolog of trithorax, activates flower homeotic genes. *Curr Biol* **13:** 627–637.

Bloch DB, Nakajima A, Gulick T, Chiche JD, Orth D, de La Monte SM, Bloch KD. 2000. Sp110 localizes to the PML-Sp100 nuclear body and may function as a nuclear hormone receptor transcriptional coactivator. *Mol Cell Biol* **20:** 6138–6146.

Bottomley MJ, Collard MW, Huggenvik JI, Liu Z, Gibson TJ, Sattler M. 2001. The SAND domain structure defines a novel DNA-binding fold in transcriptional regulation. *Nat Struct Biol* **8:** 626–633.

Bowman JL, Smyth DR, Meyerowitz EM. 1989. Genes directing flower development in *Arabidopsis*. *Plant Cell* **1:** 37–52.

Calonje M, Sanchez R, Chen L, Sung ZR. 2008. EMBRYONIC FLOWER1 participates in Polycomb Group-mediated *AG* gene silencing in *Arabidopsis*. *Plant Cell* **20:** 277–291.

Carles CC, Lertpiriyapong K, Reville K, Fletcher JC. 2004. The *ULTRAPETALA1* gene functions early in *Arabidopsis* development to restrict shoot apical meristem activity, and acts through *WUSCHEL* to regulate floral meristem determinacy. *Genetics* **167:** 1893–1903.

Carles CC, Choffnes-Inada D, Reville K, Lertpiriyapong K, Fletcher JC. 2005. *ULTRAPETALA1* encodes a putative SAND domain transcription factor that controls shoot and floral meristem activity in *Arabidopsis*. *Development* **132:** 897–911.

Chanvivattana Y, Bishopp A, Schubert D, Stock C, Moon Y-H, Sung ZR, Goodrich J. 2004. Interaction of Polycomb-group proteins controlling flowering in *Arabidopsis*. *Development* **131:** 5263–5276.

Ferguson BJ, Alexander C, Rossi SW, Liiv I, Rebane A, Worth CL, Wong J, Laan M, Peterson P, Jenkinson EJ, et al. 2008. AIRE's CARD revealed, a new structure for central tolerance provokes transcriptional plasticity. *J Biol Chem* **283:** 1723–1731.

Fletcher JC. 2001. The *ULTRAPETALA* gene controls shoot and floral meristem size in *Arabidopsis*. *Development* **128:** 1323–1333.

Gibson TJ, Ramu C, Gemund C, Aasland R. 1998. The APECED polyglandular autoimmune syndrome protein, AIRE-1, contains the SAND domain and is probably a transcription factor. *Trends Biochem Sci* **23:** 242–244.

Gomez-Mena C, de Folter S, Costa MM, Angenent GC, Sablowski R. 2005. Transcriptional program controlled by the floral homeotic gene *AGAMOUS* during early organogenesis. *Development* **132:** 429–438.

Goodrich J, Puangsomlee P, Martin M, Long D, Meyerowitz EM, Coupland G. 1997. A Polycomb-group gene regulates homeotic gene expression in *Arabidopsis*. *Nature* **386:** 44–51.

Hernandez-Munoz I, Lund AH, van der Stoop P, Boutsma E, Muijrers I, Verhoeven E, Nusinow DA, Panning B, Marahrens Y, van Lohuizen M. 2005. Stable X chromosome inactivation involves the PRC1 Polycomb complex and requires the histone MACROH2A1 and the CULLIN3/SPOP ubiquitin E3 ligase. *Proc Natl Acad Sci* **102:** 7635–7640.

Ingham PW. 1988. The molecular genetics of embryonic pattern formation in *Drosophila*. *Nature* **335:** 25–34.

Kennison JA. 1995. The Polycomb and trithorax group proteins of *Drosophila*: *Trans*-regulators of homeotic gene function. *Annu Rev Genet* **29:** 289–303.

Klymenko T, Muller J. 2004. The histone methyltransferases Trithorax and Ash1 prevent transcriptional silencing by Polycomb group proteins. *EMBO Rep* **5:** 373–377.

Lenhard M, Bohnert A, Jurgens G, Laux T. 2001. Termination of stem cell maintenance in *Arabidopsis* floral meristems by interactions between *WUSCHEL* and *AGAMOUS*. *Cell* **105:** 805–814.

Li B, Carey M, Workman JL. 2007. The role of chromatin during transcription. *Cell* **128:** 707–719.

Lohmann JU, Hong RL, Hobe M, Busch MA, Parcy F, Simon R, Weigel D. 2001. A molecular link between stem cell regulation and floral patterning in *Arabidopsis*. *Cell* **105:** 793–803.

Mizukami Y, Ma H. 1992. Ectopic expression of the floral homeotic gene *AGAMOUS* in transgenic *Arabidopsis* plants alters floral organ identity. *Cell* **71:** 119–131.

Papp B, Muller J. 2006. Histone trimethylation and the maintenance of transcriptional ON and OFF states by trxG and PcG proteins. *Genes & Dev* **20:** 2041–2054.

Petruk S, Sedkov Y, Riley KM, Hodgson J, Schweisguth F, Hirose S, Jaynes JB, Brock HW, Mazo A. 2006. Transcription of *bxd* noncoding RNAs promoted by Trithorax represses *Ubx* in *cis* by transcriptional interference. *Cell* **127:** 1209–1221.

Pfluger J, Wagner D. 2007. Histone modifications and dynamic regulation of genome accessibility in plants. *Curr Opin Plant Biol* **10:** 645–652.

Pien S, Fleury D, Mylne JS, Crevillen P, Inze D, Avramova Z, Dean C, Grossniklaus U. 2008. *ARABIDOPSIS* TRITHORAX1 dynamically regulates *FLOWERING LOCUS C* activation via histone 3 lysine 4 trimethylation. *Plant Cell* **20:** 580–588.

Pitkänen J, Doucas V, Sternsdorf T, Nakajima T, Aratani S, Jensen K, Will H, Vähämurto P, Ollila J, Vihinen M, et al. 2000. The autoimmune regulator protein has transcriptional transactivating properties and interacts with the common coactivator CREB-binding protein. *J Biol Chem* **275:** 16802–16809.

Saleh A, Al-Abdallat A, Ndamukong I, Alvarez-Venegas R, Avramova Z. 2007. The *Arabidopsis* homologs of trithorax (ATX1) and enhancer of zeste (CLF) establish 'bivalent chromatin marks' at the silent *AGAMOUS* locus. *Nucleic Acids Res* **35:** 6290–6296.

Schubert D, Clarenz O, Goodrich J. 2005. Epigenetic control of plant development by Polycomb-group proteins. *Curr Opin Plant Biol* **8:** 553–561.

Schubert D, Primavesi L, Bishopp A, Roberts G, Doonan J, Jenuwein T, Goodrich J. 2006. Silencing by plant Polycomb-group genes requires dispersed trimethylation of histone H3 at lysine 27. *EMBO J* **25:** 4638–4649.

Schuettengruber B, Chourrout D, Vervoort M, Leblanc B, Cavalli G. 2007. Genome regulation by polycomb and trithorax proteins. *Cell* **128:** 735–745.

Schuettengruber B, Ganapathi M, Leblanc B, Portoso M, Jaschek R, Tolhuis B, van Lohuizen M, Tanay A, Cavalli G. 2009. Functional anatomy of polycomb and trithorax chromatin landscapes in *Drosophila* embryos. *PLoS Biol* **7:** e1000013. doi: 10.1371/journal.pbio.1000013.

Sieburth LE, Meyerowitz EM. 1997. Molecular dissection of the *AGAMOUS* control region shows that cis elements for spatial regulation are located intragenically. *Plant Cell* **9:** 355–365.

Sun B, Xu Y, Ng K-H, Ito T. 2009. A timing mechanism for stem cell maintenance and differentiation in the *Arabidopsis* floral meristem. *Genes & Dev* **23:** 1791–1804.